Accepted in Engineering Research express on 19th September 2023

Evaluating the elastic behaviour of Boron Nitride nanotube (BNNT) reinforced Phenolic nanocomposites

Sumit Kumar Sinha[1], Dinesh Kumar[1], Saurav Goel[2,3] and Amar Patnaik[1,*]

[1] Department of Mechanical Engineering, Malaviya National Institute of Technology, Jaipur 302017, India
[2] School of Engineering, London South Bank University, 103 Borough Road, London, SE1 0AA, UK
[3] Department of Mechanical Engineering, University of Petroleum and Energy Studies, Dehradun, 248007, India

***E-mail: apatnaik.mech@mnit.ac.in**

Abstract

The present analysis concerns investigation of the elastic behavior of boron nitride nanotube (BNNT)-reinforced phenolic nanocomposite using molecular dynamics (MD) simulations. In the investigation, an armchair BNNT with chiral vectors (10, 10) was used as reinforcement and novolac-type phenolic chains and formaldehyde mixture was used as a matrix. The crosslinking of phenolic chains and formaldehyde mixture was achieved to obtain the three-dimensional crosslinked structure reinforced with BNNT. In addition to the tensile elastic modulus, the glass transition temperature was evaluated for the bulk phenolic resin and the nanocomposite using the density-temperature relationship. Based on the results, it was concluded that 6.8 % (volume fraction) of BNNT can enhance the elastic modulus of the composite by ~15 times. Poisson's ratio was found to be independent of the mixing ratio. It was also observed that reinforcement with BNNT can enhance the glass transition temperature of the nanocomposite. Continuum-based rule of mixture showed a good correlation with the MD predictions.

Keywords: BNNT; Phenolic Resins; Elastic Modulus; Poisson's Ratio; Glass Transition Temperature.

1. Introduction

Carbon nanotubes (CNTs) have revolutionized the field of nanotechnology with their discovery in 1991 by Iijima [1]. The extraordinary mechanical [2], electrical [3] and thermal [4] properties they possess have now stretched the search landscape to different materials apart from carbon, which include the like of boron nitride, being the second

hardest material after diamond. A series of efforts in this direction led to the first theoretical prediction about BNNTs by Rubio et al. [5] in 1994 which followed the first experimental realization of DWBNNT by Chopra et al. [6] in 1995 and a further experimental efforts led to the synthesis of SWBNNNT using arc discharge [7] and chemical substitution reactions [8]. Despite similar hexagonal structures, BNNTs in contrast to CNTs show different behaviour due to the differences in the covalent bonding characteristics of the B-N and C-C bonds [9]. In fact, BNNTs are superior to CNTs in terms of their oxidation resistance [10-12]. Moreover, BNNTs also reported to have superior mechanical [12-16], electrical [15] and chemical [11, 17] properties in some instances. Due to the remarkable properties, high aspect ratio, high chemical inertness and good oxidation resistant, BNNTs possess an immense potential to replace CNTs as reinforcement materials in polymer matrix to develop aerospace components like thermal protection system (TPS).

Experimental efforts to gain insights into the mechanical properties of such complex material systems are cost and time intensive [18-23], and therefore, scientists have routinely employed continuum and atomistic-based computational approaches to predict the mechanical behaviour of nanocomposite material systems.

Zhi et al. [18] predicted the mechanical and thermal behaviour of Polymethyl methacrylate (PMMA)-BN nanotube (BNNT) composites and observed that 1 % wt. fraction of BNNT in a polymer greatly enhances the elastic modulus of the matrix by 19 %. In addition, thermal stability and glass transition temperature (T_g) were also seen to improve. Zhang and Peng [19] performed MD simulations based pull-out test to characterise the interfacial behaviour of BN-CNT reinforced polyethylene (PE) nanocomposite. Their results indicated 90 % improved in the interfacial shear strength (ISS) when compared to the conventional CNT reinforced nanocomposite. Singh and Kumar [21] studied the effect of temperature on the elastic behaviour and interface of CNT-PE nanocomposite. Their results indicated that the use of small wt% of CNT in PE matrix, greatly enhances the elastic and T_g of the polymer, however, with the increase in temperature, the elastic modulus of nanocomposite and its interface drops suddenly. Han and Elliott [22] studied the elastic behavior of CNT reinforced polymer nanocomposite and reported the elastic modulus as 94.6 GPa and 138.9 GPa for 12 % and 17 % volume fractions of CNT, respectively. Wang et al. [24] studied the thermal

conductivity and mechanical performance of boron nitride nanosheets (BNNS) based epoxy adhesives and found that addition of 1 wt. % BNNS in epoxy enhances the Young's modulus, lap shear strength, fracture toughness and energy release rate by 69 %, 31 %, 122 % and 118 %, respectively. Lago et al. [25] studied the dependence of the polycarbonate mechanical performances on boron nitride fakes morphology and observed the difference in Young's modulus of 56 MPa, being the increment, compared to pristine polycarbonate with 0.1 wt. % of loading. Tank et al. [26] studied the mechanical performance of BNNT-reinforced ceramic composite and observed a significant improvements of 55 % in bending strength, 72 % in bending modulus and 63 % in thermal diffusivity with just 0.1 wt. % addition of BNNT.

It is evident from the reported literatures that scant literature exist concerning MD studies on the elastic behavior of BNNT reinforced polymer nanocomposite and there is barely any study reported on elastic behaviour of BNNT reinforced phenolic nanocomposite. In the growing efforts in this direction, this work adds to the extant understanding about these material systems by reporting the elastic behaviour of BNNT-reinforced phenolic nanocomposites.

2. Atomistic modelling and simulation

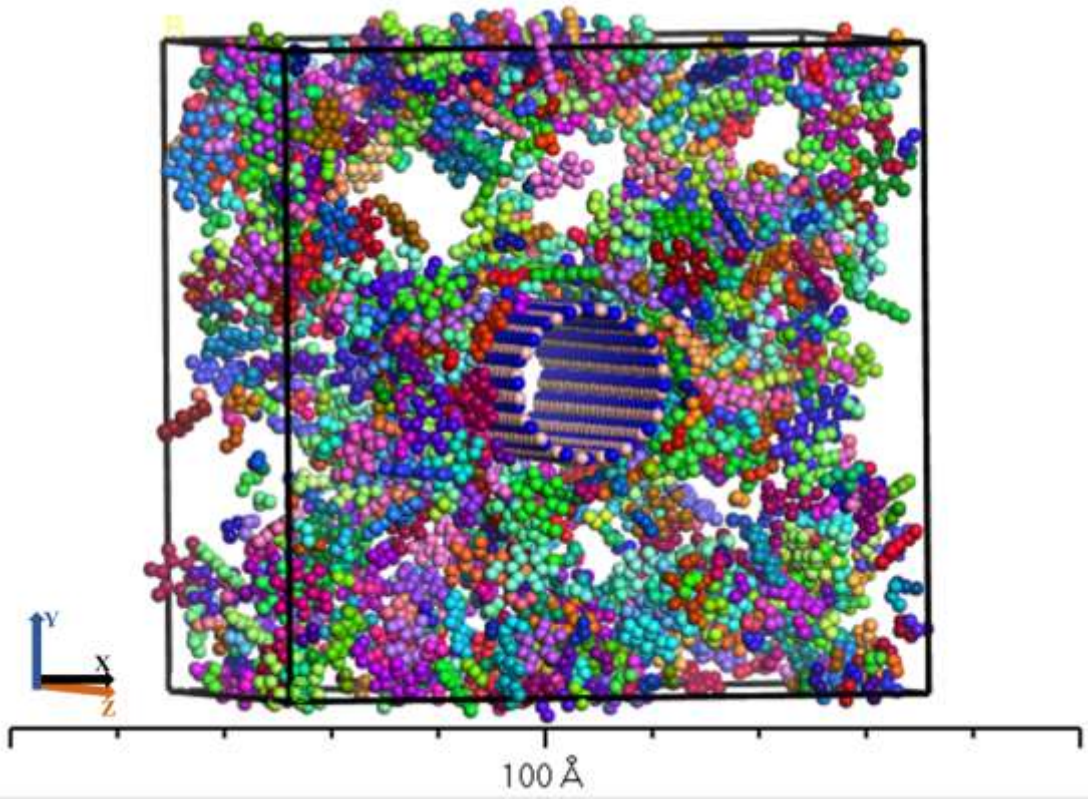

Figure 1. Atomistic model of the BNNT-reinforced phenolic nanocomposite developed in this work.

The modelling began with the construction of armchair BNNT with chiral vector (10, 10) at the center of a periodic simulation unit cell (46 Å × 46 Å × 60.11 Å) with its longitudinal axis in z-direction as shown in Fig. 1. Subsequently, 50 novolac-type phenolic chains were packed with monomers of formaldehyde into the simulation cell to model a mixture of BNNT, phenolic chain and formaldehyde. The target density was intentionally kept being low (0.6 g cm^{-3}) to ensure homogeneous mixing of phenolic chain and formaldehydes during the equilibration process. Thereafter, the total potential energy of the structure was minimised using steepest descent algorithm [27] with energy convergence tolerance of 0.001 kcal mol^{-1}. The model construction was done using the commercially available material studio 8.0 [28].

After obtaining the initial atomistic configuration, MD simulations were performed with an open source code, LAMMPS (Large Atomistic/Molecular Massively Parallel Simulator) [29]. To do so a hybrid force-field scheme (combination of polymer consistent force field (PCFF) [30] and Tersoff potential [31]) was implemented. The system's temperature and pressure were regulated by implementing Nóse-Hoover thermostat [32, 33] and barostat [33, 34], respectively. Periodic boundary conditions were implemented in all the three directions. A cut-off radius of 15 Å was used. The long-range interactions contribution to the pressure and energy beyond cut-off distance were computed via utilising the tail correction and particle-particle-particle mesh algorithm [35].

Initially, the total potential energy of the atomistic structure was minimised using the fire algorithm [36] with an energy convergence tolerance of 0.001 kcal mol^{-1}. Thereafter, the structure in LAMMPS was simulated using NVT followed by NPT ensemble. This was done to ensure proper mixing of phenolic chain and formaldehyde mixture, while BNNT was maintained to remain at the center of the simulation cell. The improper mixing would have made a negative impact on the emerging three-dimensional networks (like reduced degree of crosslinking) and inaccurate predictions. To this end, initially the structure was subjected to annealing to a target temperature of 600 K with a heating rate of 1 K ps^{-1} using NVT ensemble MD simulation. The structure was kept at this temperature for another 300 ps before cooling it to 450 K with the cooling rate of 1 K ps^{-1}. Thereafter, the structure was subjected to isobaric-isothermal

(NPT) ensemble MD simulations at temperature and pressure of 450 K and 1 atm, respectively, to get the well mixed equilibrated structure.

The modified crosslinking algorithm based on dynamic method of curing was utilised for curing of the phenolic chains and formaldehyde mixture. The structure was cured in iterative manner and in each iteration, limited set of reactions were allowed to occur (25 reactions per iteration). The initial search radius was kept as 3.5 Å which later on increases dynamically (increment of 0.5 Å) based on the availability of reaction sites. A single crosslink iteration consists of identification of reactive sites, polymerization (curing), multi-step relaxation and heating/cooling cycles. After completion of every crosslinking iteration, the structure was subjected to isothermal-isobaric (NPT) ensemble MD simulations to let the system evolve dynamically. The charges of the newly formed bonds were updated during the polymerization stage by using the bond increment charging algorithm of the PCFF force-field. The topologies are also updated during the same stage. After obtaining the desired level of degree of crosslinking, elastic behaviour of the BNNT-reinforced crosslinked phenolic nanocomposite was estimated. T_g of the obtained nanocomposite was also evaluated using density-temperature relationship. Continuum-based rule of mixture (ROM) was utilised in the end to validate the results obtained from the MD simulations.

3. Results and Discussions

3.1. Glass Transition Temperature (T_g)

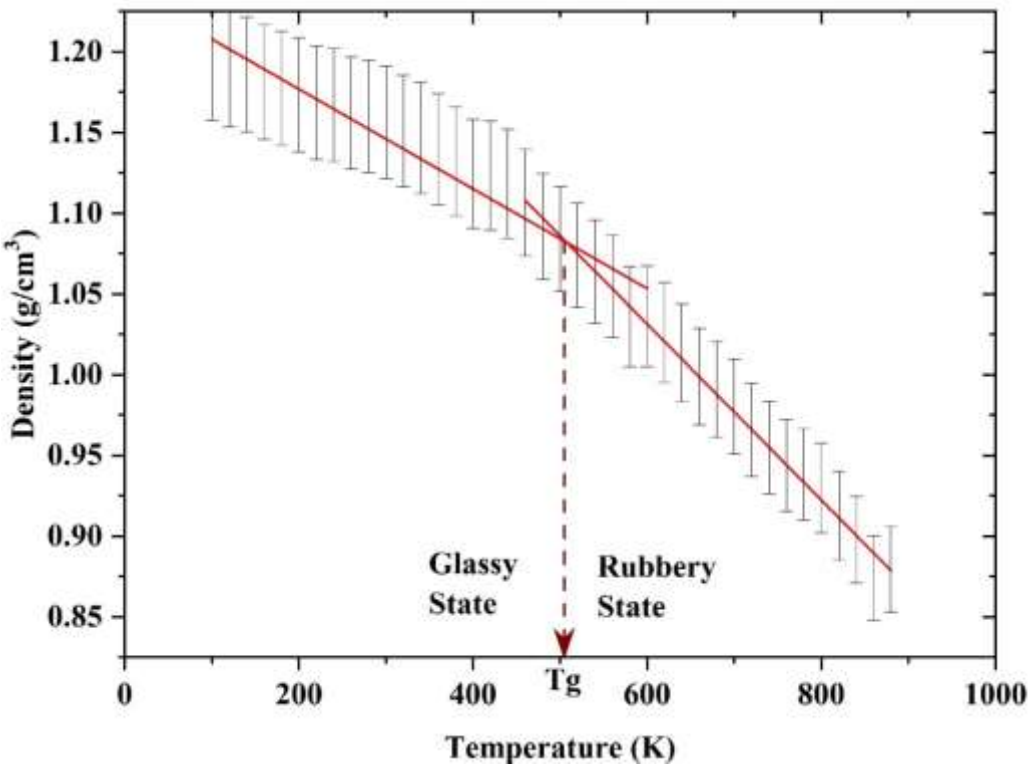

(a)

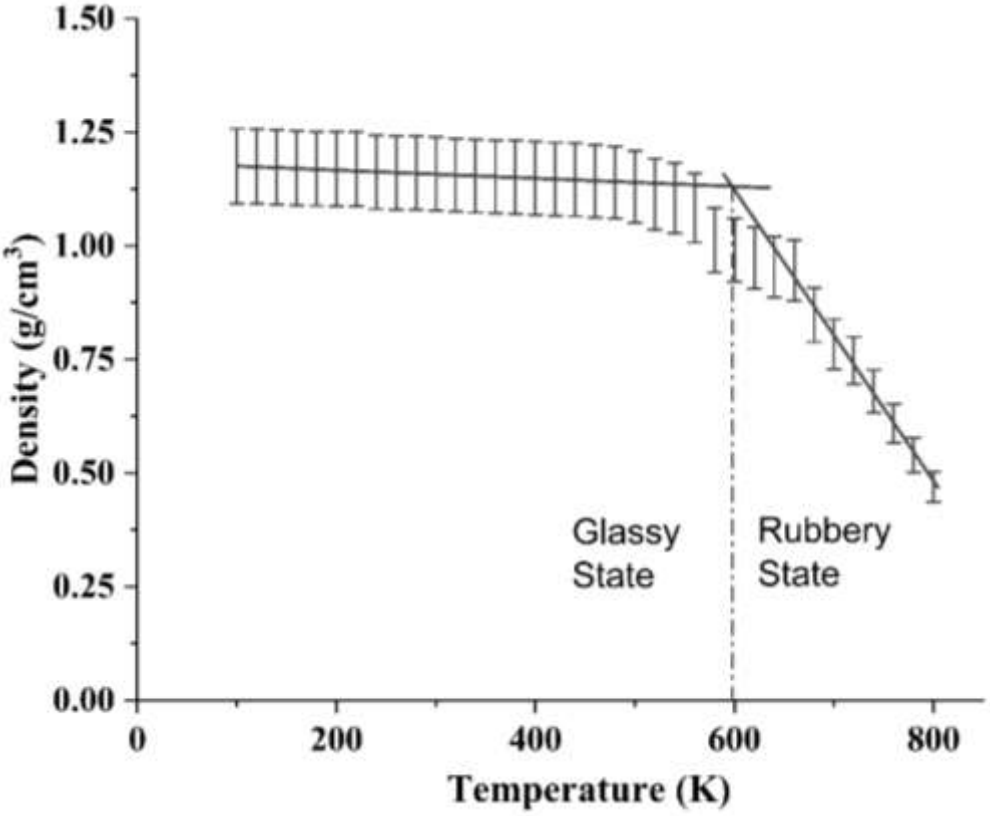

(b)

Figure 2. Density vs. Temperature curves (a) Bulk phenolic resin matrix (b) BNNT-reinforced phenolic nanocomposite.

The glass transition temperature (T_g) of the bulk polymer matrix/nanocomposite can be effectively evaluated by using the MD simulation. The previously published literature suggests two methods- temperature dependent density and temperature dependent specific volume. Majority of those papers [21, 37-39] have used temperature dependent density to predict the glass transition temperature (T_g). Few articles [40-42] also used temperature dependent specific volume to predict the T_g. However, Varshney et al. [39] have shown that, both methods predict the same T_g since specific volume is expressed as:

$$\upsilon = \frac{1}{\rho} \tag{1}$$

where, υ is specific volume and ρ is density.

To evaluate the T_g of bulk phenolic resin/Boron Nitride nanotube (BNNT) reinforced phenolic nanocomposite, the equilibrated structure of the phenolic resin/nanocomposite was slowly cooled down from a high temperature of 800 K to a low temperature of 100 K with a cooling rate of 0.5 K ps^{-1} in an anisotropic (NPT ensemble) cooling. While cooling, the variations of the simulation cell were totally decoupled in all the three directions. The structures were cooled in the interval of 20 K and at each interval of temperature, the structures were simulated for 300 ps in a constant pressure (NPT) ensemble. The density values (data points) were noted for every picosecond. Based on the 300 data points, evaluated from the 300 ps trajectory, the average densities of the structures were evaluated at each interval of temperature. The change in the density of the structure was monitored over a broad range of temperature (i.e., from 800 K to 100 K). Finally, from the values of densities obtained at various temperatures, the density versus temperature curves along with estimated error bars (5% of data), was plotted. The linear fitting function was used for the initial (i.e., glassy or brittle) and final (i.e., rubbery or amorphous) regions of the density vs. temperature curves and the intersection point of the two fits was taken as the T_g, as shown in Fig. 2. The T_g of the parent matrix and that of the BNNT reinforced phenolic nanocomposite were estimated to be ~ 514 K and ~ 592 K, respectively as shown in Fig. 2. Several research articles [31, 34-36] confirms that, the T_g of bulk phenolic resin (matrix) falls in the range of 500 K to 600 K, depending on the molecular weight and degree of cross-linking of the resin. Zhi et al. [18] showed that the reinforcement with

BNNT in the bulk phenolic resin (matrix) significantly enhances the T_g of the nanocomposite in comparison to the bulk phenolic resin.

T_g of the BNNT-reinforced nanocomposite was also evaluated from temperature dependent specific volume as shown as Fig. 3. It can be seen that the results obtained from both methods are identical.

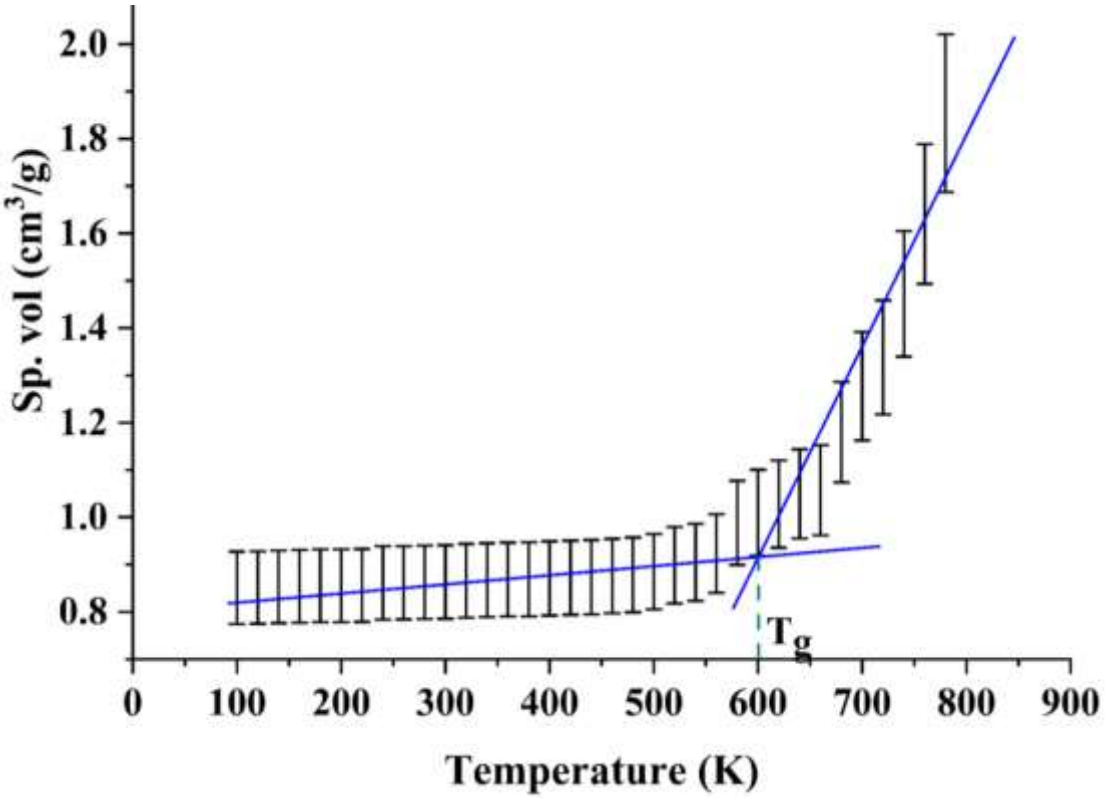

Figure 3. Sp. Vol. vs temperature plot for BNNT nanocomposite. The intersection of the line predict the glass transition temperature (T_g) as ~ 600 K.

The increase in temperature towards the glass transition temperature sets the transition from a glassy phase to a rubbery phase. Arbe et al. [43] considered the T_g in polymer as homogeneous scenario where some other researchers [44-48] have considered this as a heterogeneous scenario with second order phase transition. The growth from glassy state to rubbery phase was considered via a thermodynamic driving force in the second order phase transition theory [refer [48]]. When considering the bulk phenolic resin only, the resistance to this thermodynamic driving force is only offered by the phenolic chains while in the case of BNNT-reinforced phenolic nanocomposite, there is an additional resistance force that arises from the energy dissipation of interfacial energy and the involvement of BNNT nanofiller. Therefore, Tg of the bulk

phenolic resin matrix is about 500K while the Tg of BNNT-reinforced phenolic nanocomposite is about 600 K. Ramanathan et al. [49] have also shown in their study that addition of nanofiller restrained the mobility of polymer chains and therefore higher Tg was obtained when compared to the parent matrix.

3.2. Elastic modulus of pure phenolic resin and BNNT

To evaluate the tensile elastic modulus, the structure was first relaxed to obtain mass density in the range of 1.0-1.2 g cm^{-3}. The elastic modulus for pure phenolic resin at a temperature of 300 K was estimated as 3.9 GPa (depending on the molecular weight and degree of crosslinking). The reported results for pure phenolic resin in literature were seen to be in the range of 3.5 GPa to 5.5 GPa [50, 51].

The elastic modulus of BNNT with chiral vector (10, 10) having diameter of 13.81 Å was also estimated using the same procedure of MD simulations at a temperature of 300 K. The elastic modulus for BNNT was obtained as 800 GPa which was seen to be in close proximity of the value of 850 GPa reported by Suryavanshi et al. [52].

3.3. Stress-Strain relation and elastic modulus of the nanocomposite

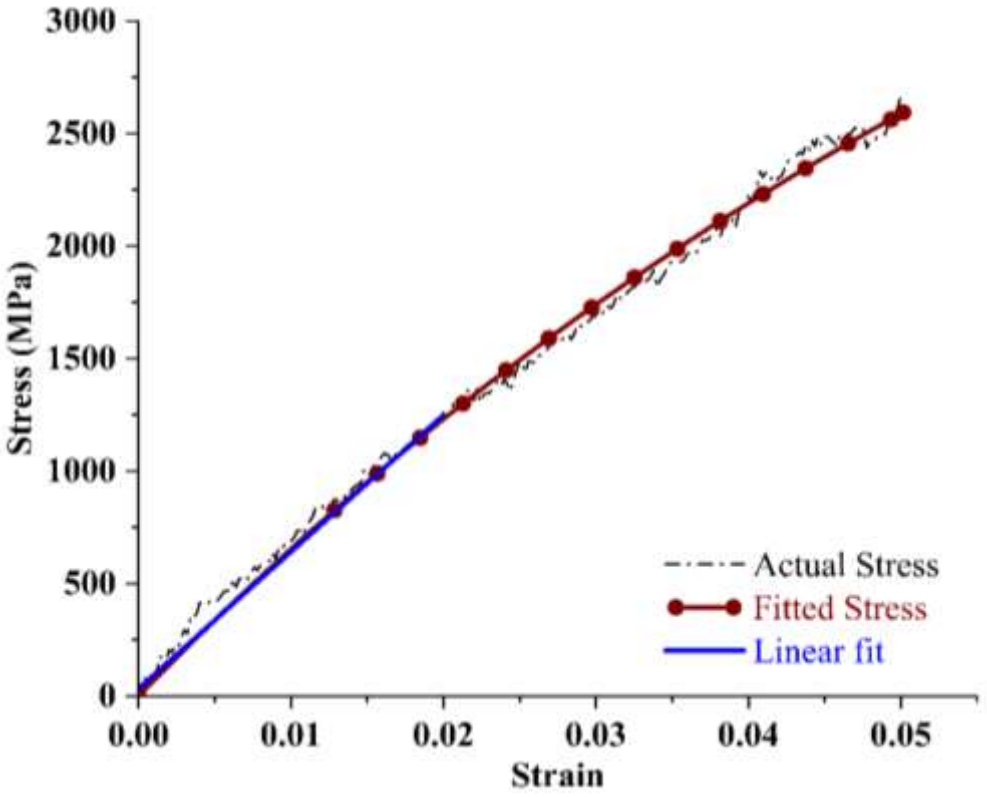

Figure 4. Stress-strain curve obtained for BNNT-reinforced phenolic nanocomposite.

In this study, the stress-strain behavior of BNNT-reinforced phenolic nanocomposite was estimated by performing uniaxial tensile deformation using LAMMPS.

To estimate the stress-strain response of the structure, non-equilibrium MD (NEMD) simulation was performed with a constant strain rate of 2×10^8 s^{-1}, applied in the direction of the longitudinal axis (i.e., z-direction) of the simulation cell. To simulate the dynamic behaviour of the other two directions with respect to strain, an ambient pressure of 1 atm was applied. The kinetic response of the atoms with respect to applied strain was monitored at a constant temperature of 300 K using an anisotropic coupling. The stresses were calculated at every step of applied strain using virial stress tensor defined by Eq. (1). The response of the stresses with respect to applied strain was plotted in the form of stress-strain curve, as shown in Fig. 4. A polynomial curve was fitted. A linear fit of up to 2% of strain was fitted to obtain the slope of the stress-strain curve within elastic limit. The elastic modulus of the BNNT-reinforced phenolic nanocomposite from this linear slope was approximated to be 60.79 GPa.

$$\sigma_{ij} = \frac{\sum_K^N m_K v_{Ki} v_{Kj}}{V} + \frac{\sum_K^N f_{Kj} r_{Ki}}{V} \quad (2)$$

3.4. Poisson's ratio

The simulation cell lengths were seen to contract in the direction transverse to the direction of applied strain. This is due to the well-known Poisson's effect. To estimate the Poisson's ratio in the present study, the contraction of simulation cell lengths was recorded with respect to the elongation of the simulation cell length in the direction of applied strain and this trend is shown in Fig. 5. The direction of applied strain was considered as the longitudinal axis whereas the directions perpendicular to it were considered as the transverse axis. Longitudinal/transverse strain was calculated as the change in the simulation cell length with respect to original length. A curve was plotted for the transverse vs. longitudinal strain, as shown in Fig. 6. The slope of this curve predicted the Poisson's ratio of the BNNT-reinforced nanocomposite as 0.36.

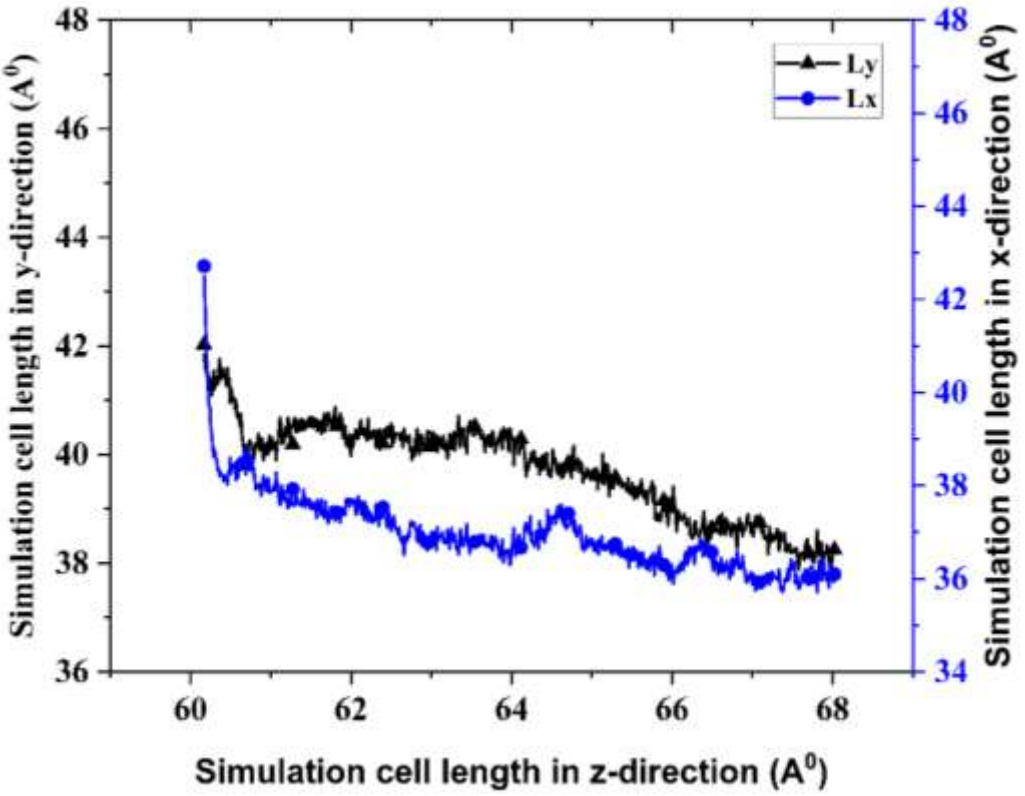

Figure 5. The change in simulation cell length in x- and y-direction with respect to change in cell length in z-direction.

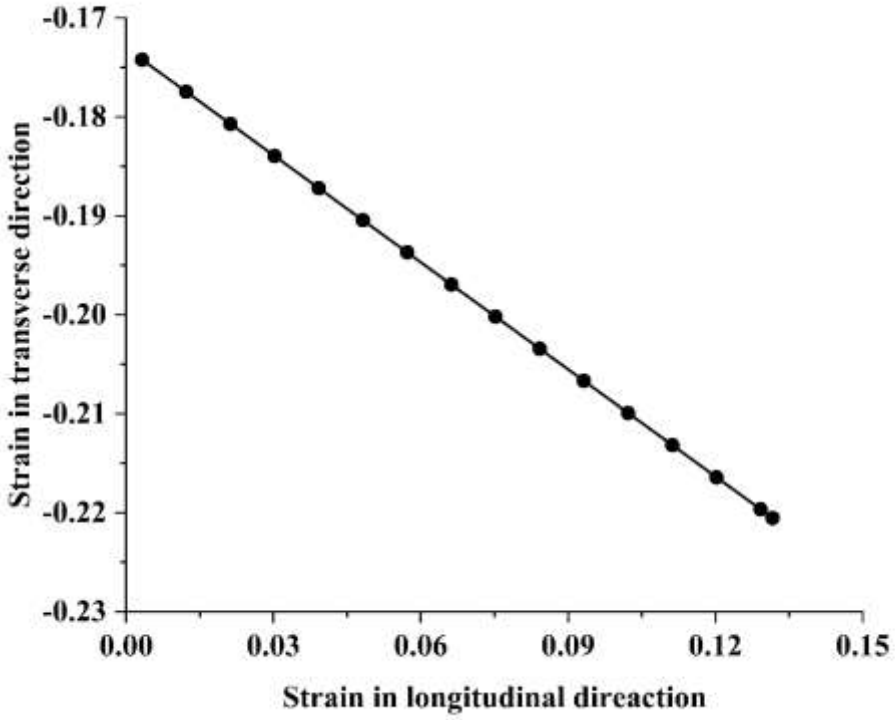

Figure 6. Longitudinal strain vs. transverse strain. The slope of this curve can be used to obtain Poisson's ratio.

3.5. Comparison of MD results with continuum-based Rule of Mixture (ROM):

The elastic properties obtained for BNNT, phenolic resin (matrix) and its nanocomposite obtained from the MD simulations were compared with the continuum-based Rule of Mixture (ROM). Based on the theory of continuum mechanics, ROM assumes that there is a perfect bonding between reinforcement and matrix. The elastic modulus of the BNNT-reinforced phenolic nanocomposite can be estimated using compatibility equations for strains and equilibrium equations for stresses [53].

Mathematically,

$$\mathrm{E_{nc}} = \mathrm{V_f^{BNNT}E_{BNNT}} + \mathrm{V_f^{m}E_m} \tag{3}$$

where, E_{nc}, E_{BNNT} and E_m represents the elastic moduli of the nanocomposite, BNNT and the phenolic resin (matrix), respectively, and V_f^{BNNT} and V_f^m represents the volume fractions of BNNT and the phenolic resin matrix in the nanocomposite, respectively. Further, the volume fractions of BNNT and pure phenolic resin matrix must satisfy the following conditions:

$$V_f^{BNNT} + V_f^m = 1 \tag{4}$$

Initially, the BNNT (V_f^{BNNT}) was modeled as solid BNNT based on the basic assumption (i.e., continuum reinforcement) of micromechanics of ROM. To calculate the equivalent radius of solid BNNT (r_{sBNNT}), the cross-sectional area of the hollow BNNT is taken equal to that of solid BNNT, as reported by Rafiee and Madhavi [54]. The equations for radius and volume fraction of solid BNNT can be derived as:

$$\mathrm{r_{sBNNT}} = \sqrt{2\mathrm{r_{BNNT}t_{BNNT}}} \tag{5}$$

$$V_f^{BNNT} = \frac{\pi r_{sBNNT}^2}{A_{cs}} \tag{6}$$

where t_{BNNT} and r_{BNNT} are the wall-thickness and radius of hollow BNNT, respectively, and A_{cs} represents the cross-sectional area of the BNNT-reinforced phenolic nanocomposite (i.e., cross-sectional area obtained after final equilibration (NPT ensemble) of the nanocomposite.

Table 1. Validation of the results obtained from MD simulations through the rule of mixture (ROM)

BNNT (chirality)	Volume fraction V_f^{BNNT} (%)	Elastic modulus, E (GPa)			
		MD simulation estimated value			Analytical value using ROM
		Pure BNNT	Pure Phenolic resin	Nanocomposite	Nanocomposite
Single-walled (10, 10)	6.8	800	3.9	60.79	58

It can be noted from the Table 1 that the results obtained from the MD simulations and using continuum ROM comparing the elastic modulus of nanocomposites modelled in this work were fairly close which renders strong confidence in the predictions made using the MD simulations.

4. Conclusion

The present study concerns MD simulations to predict the mechanical properties such as the elastic modulus, glass transition temperature (T_g) and Poisson's ratio of a boron nitride reinforced phenolic resin nanocomposite in an effortless manner. The predicted results were validated using the continuum-based Rule of Mixture (ROM) theory. Based on the discussions offered, the following conclusions can be drawn:

1. 6.8 % volume fraction of BNNT in the phenolic resin was seen to greatly enhance the elastic behaviour of phenolic resin and its nanocomposite which was evident from the corresponding improvement seen in the mechanical properties. It was shown for instance that the T_g got improved from ~514 K to ~592 K by adding the BNNT reinforcement.
2. The Poisson's ratio was seen to be independent of the reinforcement and value remain independent to the percentage of BNNT mixed in the base material phenolic resin.

Declarations

Funding

The authors declare that no funds, grants, or other support were received during the preparation of this manuscript.

Conflict of interest/Competing interests

The authors have no relevant financial or non-financial interests to disclose.

Author Contributions

Sumit Kumar Sinha: Conceptualization, Methodology, Software, Formal analysis, Writing-Original draft preparation**; Dinesh Kumar:** Supervision; **Amar Patnaik:** Writing- review & editing, Validation and Supervision; **Saurav Goel:** Writing- review & editing, Validation and Supervision.

Acknowledgements

Sumit Kumar Sinha acknowledge the HPC support from the computing center of Indian Institute of Technology Kanpur (IIT Kanpur).

References

[1] Iijima, S., 1991. Helical microtubules of graphitic carbon. *nature*, *354*(6348), pp.56-58.
[2] Ruoff, R.S. and Lorents, D.C., 1995. Mechanical and thermal properties of carbon nanotubes. *carbon*, *33*(7), pp.925-930.
[3] Rochefort, A., Avouris, P., Lesage, F. and Salahub, D.R., 1999. Electrical and mechanical properties of distorted carbon nanotubes. *Physical Review B*, *60*(19), p.13824.
[4] Kothari, R., Kundalwal, S.I. and Sahu, S.K., 2018. Transversely isotropic thermal properties of carbon nanotubes containing vacancies. *Acta Mechanica*, *229*, pp.2787-2800.
[5] Rubio, A., Corkill, J.L. and Cohen, M.L., 1994. Theory of graphitic boron nitride nanotubes. *Physical Review B*, *49*(7), p.5081.
[6] Chopra, N.G., Luyken, R.J., Cherrey, K., Crespi, V.H., Cohen, M.L., Louie, S.G. and Zettl, A., 1995. Boron nitride nanotubes. *science*, *269*(5226), pp.966-967.
[7] Loiseau, A., Willaime, F., Demoncy, N., Hug, G. and Pascard, H., 1996. Boron nitride nanotubes with reduced numbers of layers synthesized by arc discharge. *Physical review letters*, *76*(25), p.4737.
[8] Golberg, D., Bando, Y., Han, W., Kurashima, K. and Sato, T., 1999. Single-walled B-doped carbon, B/N-doped carbon and BN nanotubes synthesized from single-walled carbon nanotubes through a substitution reaction. *Chemical Physics Letters*, *308*(3-4), pp.337-342.
[9] Chopra, N.G. and Zettl, A., 1998. Measurement of the elastic modulus of a multi-wall boron nitride nanotube. *Solid State Communications*, *105*(5), pp.297-300.
[10] Lin, Y., Bunker, C.E., Fernando, K.S. and Connell, J.W., 2012. Aqueously dispersed silver nanoparticle-decorated boron nitride nanosheets for reusable, thermal oxidation-resistant surface enhanced Raman spectroscopy (SERS) devices. *ACS applied materials & interfaces*, *4*(2), pp.1110-1117.

[11] Turhan, E.A., Pazarçeviren, A.E., Evis, Z. and Tezcaner, A., 2022. Properties and applications of boron nitride nanotubes. *Nanotechnology*, *33*(24), p.242001.
[12] Zhang, Y., Niu, H., Liyun, W., Wang, N., Xu, T., Zhou, Z., Xie, Y., Wang, H., He, Q., Zhang, K. and Yao, Y., 2021. Fabrication of thermally conductive polymer composites based on hexagonal boron nitride: recent progresses and prospects. *Nano Express*, *2*(4), p.042002.
[13] Chen, Y., Zou, J., Campbell, S.J. and Le Caer, G., 2004. Boron nitride nanotubes: Pronounced resistance to oxidation. *Applied physics letters*, *84*(13), pp.2430-2432.
[14] Griebel, M. and Hamaekers, J., 2007. Molecular dynamics simulations of boron-nitride nanotubes embedded in amorphous Si-BN. *Computational materials science*, *39*(3), pp.502-517.
[15] Vaccarini, L., Goze, C., Henrard, L., Hernandez, E., Bernier, P. and Rubio, A., 2000. Mechanical and electronic properties of carbon and boron–nitride nanotubes. *Carbon*, *38*(11-12), pp.1681-1690.
[16] Bedi, D., Sharma, A., Sharma, S. and Tiwari, S.K., 2022, July. Molecular Dynamics Simulation of Carbon and Boron Nitride nanotubes: Tensile and Compressive Behavior. In *IOP Conference Series: Materials Science and Engineering* (Vol. 1248, No. 1, p. 012101). IOP Publishing.
[17] Golberg, D., Bando, Y., Kurashima, K. and Sato, T., 2001. Synthesis and characterization of ropes made of BN multiwalled nanotubes. *Scripta Materialia*, *44*(8-9), pp.1561-1565.
[18] Zhi, C.Y., Bando, Y., Wang, W.L., Tang, C.C., Kuwahara, H. and Golberg, D., 2008. Mechanical and thermal properties of polymethyl methacrylate-BN nanotube composites. *Journal of Nanomaterials*, *2008*.
[19] Zhang, J. and Peng, X., 2017. Superior interfacial mechanical properties of boron nitride-carbon nanotube reinforced nanocomposites: A molecular dynamics study. *Materials Chemistry and Physics*, *198*, pp.250-257.
[20] Wang, Z.J., Kwon, D.J., Gu, G.Y., Lee, W.I., Park, J.K., DeVries, K.L. and Park, J.M., 2014. Ablative and mechanical evaluation of CNT/phenolic composites by thermal and microstructural analyses. *Composites Part B: Engineering*, *60*, pp.597-602.
[21] Singh, A. and Kumar, D., 2018. Effect of temperature on elastic properties of CNT-polyethylene nanocomposite and its interface using MD simulations. *Journal of Molecular Modeling*, *24*, pp.1-11.
[22] Han, Y. and Elliott, J., 2007. Molecular dynamics simulations of the elastic properties of polymer/carbon nanotube composites. *Computational Materials Science*, *39*(2), pp.315-323.
[23] Singh, A. and Kumar, D., 2019. Effect of functionalization on the elastic behavior of graphene nanoplatelet-PE nanocomposites with interface consideration using a multiscale approach. *Mechanics of Materials*, *132*, pp.18-30.
[24] Wang, S., Xue, H., Araby, S., Demiral, M., Han, S., Cui, C., Zhang, R. and Meng, Q., 2021. Thermal conductivity and mechanical performance of hexagonal boron nitride nanosheets-based epoxy adhesives. *Nanotechnology*, *32*(35), p.355707.
[25] Lago, E., Toth, P.S., Gentiluomo, S., Thorat, S.B., Pellegrini, V. and Bonaccorso, F., 2021. Dependence of the polycarbonate mechanical performances on boron nitride flakes morphology. *Journal of Physics: Materials*, *4*(4), p.045002.

[26] Tank, M., De Leon, A., Huang, W., Patadia, M., Degraff, J. and Sweat, R., 2023. Manufacturing of stereolithographic 3D printed boron nitride nanotube-reinforced ceramic composites with improved thermal and mechanical performance. *Functional Composites and Structures*, *5*(1), p.015001.
[27] Fletcher, R. and Powell, M.J., 1963. A rapidly convergent descent method for minimization. *The computer journal*, *6*(2), pp.163-168.
[28] Material Studio 8.0. Accelrys Inc, San Diego.
[29] Thompson, A.P., Aktulga, H.M., Berger, R., Bolintineanu, D.S., Brown, W.M., Crozier, P.S., in't Veld, P.J., Kohlmeyer, A., Moore, S.G., Nguyen, T.D. and Shan, R., 2022. LAMMPS-a flexible simulation tool for particle-based materials modeling at the atomic, meso, and continuum scales. *Computer Physics Communications*, *271*, p.108171.
[30] Sun, H., Mumby, S.J., Maple, J.R. and Hagler, A.T., 1994. An ab initio CFF93 all-atom force field for polycarbonates. *Journal of the American Chemical society*, *116*(7), pp.2978-2987.
[31] Kınacı, A., Haskins, J.B., Sevik, C. and Çağın, T., 2012. Thermal conductivity of BN-C nanostructures. *Physical Review B*, *86*(11), p.115410.
[32] Nosé, S., 1984. A unified formulation of the constant temperature molecular dynamics methods. *The Journal of chemical physics*, *81*(1), pp.511-519.
[33] Hoover, W.G., 1985. Canonical dynamics: Equilibrium phase-space distributions. *Physical review A*, *31*(3), p.1695.
[34] Hoover, W.G., 1986. Constant-pressure equations of motion. *Physical Review A*, *34*(3), p.2499.
[35] Hockney, R.W. and Eastwood, J.W., 2021. *Computer simulation using particles*. crc Press.
[36] Guénolé, J., Nöhring, W.G., Vaid, A., Houllé, F., Xie, Z., Prakash, A. and Bitzek, E., 2020. Assessment and optimization of the fast inertial relaxation engine (fire) for energy minimization in atomistic simulations and its implementation in lammps. *Computational Materials Science*, *175*, p.109584.
[37] Monk, J.D., Bucholz, E.W., Boghozian, T., Deshpande, S., Schieber, J., Bauschlicher Jr, C.W. and Lawson, J.W., 2015. Computational and experimental study of phenolic resins: Thermal–mechanical properties and the role of hydrogen bonding. *Macromolecules*, *48*(20), pp.7670-7680.
[38] Komarov, P.V., Yu-Tsung, C., Shih-Ming, C., Khalatur, P.G. and Reineker, P., 2007. Highly cross-linked epoxy resins: an atomistic molecular dynamics simulation combined with a mapping/reverse mapping procedure. Macromolecules, 40(22), pp.8104-8113.
[39] Varshney, V., Patnaik, S.S., Roy, A.K. and Farmer, B.L., 2008. A molecular dynamics study of epoxy-based networks: cross-linking procedure and prediction of molecular and material properties. Macromolecules, 41(18), pp.6837-6842.
[40] Izumi, A., Shudo, Y., Hagita, K. and Shibayama, M., 2018. Molecular Dynamics Simulations of Cross-Linked Phenolic Resins Using a United-Atom Model. *Macromolecular Theory and Simulations*, *27*(4), p.1700103.
[41] Izumi, A., Nakao, T. and Shibayama, M., 2012. Atomistic molecular dynamics study of cross-linked phenolic resins. *Soft Matter*, *8*(19), pp.5283-5292.
[42] Monk, J.D., Haskins, J.B., Bauschlicher Jr, C.W. and Lawson, J.W., 2015. Molecular dynamics simulations of phenolic resin: Construction of atomistic models. *Polymer*, *62*, pp.39-49.

[43] Arbe, A., Colmenero, J., Monkenbusch, M. and Richter, D., 1998. Dynamics of glass-forming polymers:"Homogeneous" versus "heterogeneous" scenario. Physical review letters, 81(3), p.590.
[44] Gibbs, J.H. and DiMarzio, E.A., 1958. Nature of the glass transition and the glassy state. The Journal of Chemical Physics, 28(3), pp.373-383.
[45] Chow, T.S., 1980. Molecular interpretation of the glass transition temperature of polymer-diluent systems. Macromolecules, 13(2), pp.362-364.
[46] Sillescu, H., Böhmer, R., Diezemann, G. and Hinze, G., 2002. Heterogeneity at the glass transition: what do we know?. Journal of Non-Crystalline Solids, 307, pp.16-23.
[47] Lu, H. and Huang, W.M., 2013. On the origin of the Vogel–Fulcher–Tammann law in the thermo-responsive shape memory effect of amorphous polymers. Smart Materials and Structures, 22(10), p.105021.
[48] Xia, X., Li, J., Zhang, J. and Weng, G.J., 2021. Uncovering the glass-transition temperature and temperature-dependent storage modulus of graphene-polymer nanocomposites through irreversible thermodynamic processes. International Journal of Engineering Science, 158, p.103411.
[49] Ramanathan, T., Abdala, A.A., Stankovich, S., Dikin, D.A., Herrera-Alonso, M., Piner, R.D., Adamson, D.H., Schniepp, H.C., Chen, X.R.R.S., Ruoff, R.S. and Nguyen, S.T., 2008. Functionalized graphene sheets for polymer nanocomposites. Nature nanotechnology, 3(6), pp.327-331.
[50] Wang, Z.J., Kwon, D.J., Gu, G.Y., Lee, W.I., Park, J.K., DeVries, K.L. and Park, J.M., 2014. Ablative and mechanical evaluation of CNT/phenolic composites by thermal and microstructural analyses. *Composites Part B: Engineering*, *60*, pp.597-602.
[51] Yeh, M.K., Tai, N.H. and Liu, J.H., 2006. Mechanical behavior of phenolic-based composites reinforced with multi-walled carbon nanotubes. *Carbon*, *44*(1), pp.1-9.
[52] Suryavanshi, A.P., Yu, M.F., Wen, J., Tang, C. and Bando, Y., 2004. Elastic modulus and resonance behavior of boron nitride nanotubes. *Applied Physics Letters*, *84*(14), pp.2527-2529.
[53] Srivastava, A. and Kumar, D., 2017. A continuum model to study interphase effects on elastic properties of CNT/GS-nanocomposite. *Materials Research Express*, *4*(2), p.025036.
[54] Rafiee, R. and Mahdavi, M., 2016. Characterizing nanotube–polymer interaction using molecular dynamics simulation. *Computational Materials Science*, *112*, pp.356-363.